Electron Capture into the 4s State of H by Fast H^+ Impact on Gases*

R. H. HUGHES, H. R. DAWSON,† AND B. M. DOUGHTY‡
Department of Physics, University of Arkansas, Fayetteville, Arkansas
(Received 16 December 1966)

Cross sections have been determined for electron capture into the 4s state of atomic hydrogen by fast-proton (5–120-keV) impact on He, Ar, Ne, N_2, H_2, and O_2. Some improved measurements are reported on previously published cross sections for electron capture into the 3s state of atomic hydrogen for fast-proton impact on these gases. Above 80 keV, the cross sections for capture into the 3s and 4s states appear to be proportional to n^{-3}, where n is the principal quantum number of the final state. Secondary structure appears in the 3s and 4s excitation functions for impact on the heavier gases (Ar, Ne, N_2, and O_2) below 7 keV.

I. INTRODUCTION

IN a previous paper[1] we reported cross-section measurements for electron capture into the 3s state of H by fast-proton impact on He, Ar, Ne, N_2, O_2, and H_2. In this paper we report cross-section measurements for electron capture into the 4s state of H by fast-proton impact on these same gases along with additional 3s capture measurements and remeasurements.

The technique for measuring the 3s cross sections described in Ref. 1 involved passing a monoenergetic proton beam through a differentially pumped collision chamber which contained the target gas. Electrons were captured by the protons into various states of atomic hydrogen in this chamber. The resulting fast atoms emerged from the collision chamber into an evacuated observation chamber where the excited atoms decayed in flight. Cross sections for capture into the 3s state were determined by measuring H_α ($n=3\rightarrow 2$) radiation at a point sufficiently far from the collision chamber to ensure that only the $3s\rightarrow 2p$ transition was being observed. Those atoms excited into the short-lived 3p and 3d states contributed essentially no radiation at this point, having already decayed off.

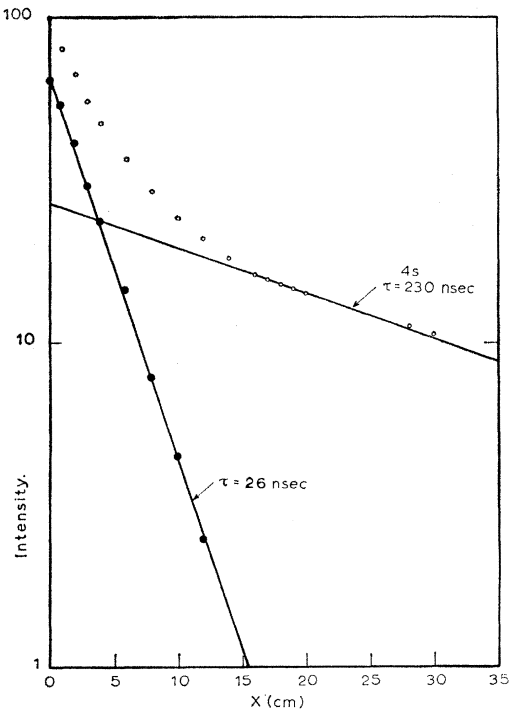

FIG. 1. Plot of H_β intensity versus distance from the beam departure aperture for 10-keV H^+ impact on Ar (beam current about 1 μA). The open circles represent the raw data while the closed circles represent the difference between the raw data and the long-lived (230-nsec) decay.

This technique is easily adapted to measuring capture into the 4s state of H. In this case measurements are made on H_β ($n=4\rightarrow 2$) radiation at a point in the observation chamber where all of the shorter-lived $n=4$ states have decayed off, leaving only the long-lived $4s\rightarrow 2p$ radiation.

In Ref. 1 some concern was indicated over the possibility of Stark mixing of certain $n=3$ states by small electric fields that might be present in the collision chamber.

As applied to this experiment, the Stark effect is considered in the following section.

II. STARK-EFFECT CONSIDERATIONS

Very small electric fields can Stark-mix certain states together.[2] Especially vulnerable to mixing are $4d_{3/2}$ with $4p_{3/2}$ states and $4f_{5/2}$ with $4d_{5/2}$ states since the energy separation between these levels is extremely small. The $4s_{1/2}$ and $4p_{1/2}$ states are separated by the Lamb shift which reduces the probability of mixing. However, the $s_{1/2}$ and $p_{1/2}$ states are more easily mixed at $n=4$ than at $n=3$ since not only is the Lamb shift smaller at $n=4$ but also the matrix elements connecting the states through the Stark effect are larger at $n=4$. (The critical field,[2] that minimum field which will fully mix the states, is 12 and 58 V/cm for the $s_{1/2}$ and $p_{1/2}$ states at $n=4$ and $n=3$, respectively.[2] The critical field for $p_{3/2}$ and $d_{3/2}$ mixing is approximately $\frac{1}{2}$V/cm and 2 V/cm at $n=4$ and $n=3$, respectively.[2])

* Research supported by the National Science Foundation.
† Present address: Physics Department, Angelo State College, San Angelo, Texas.
‡ National Aeronautics and Space Adminstration Predoctoral Trainee.
[1] R. H. Hughes, H. R. Dawson, B. M. Doughty, D. B. Kay, and C. A. Stigers, Phys. Rev. 53, (1966)
[2] H. E. Bethe and E. E. Salpeter, *Quantum Mechanics of One- and Two-Electron Systems* (Academic Press Inc., New York, 1957), p. 288.

In our previous paper we implied that electric fields exist inside the collision chamber which partially mix the $3p_{3/2}$ and $3d_{3/2}$ states. The decay of H_α radiation outside the collision chamber indicated that the fields in the observation chamber were too small to produce appreciable mixing. However, in the case of the $n=4$ level, the fields in the observation chamber can apparently produce appreciable mixing. Figure 1 shows an H_β decay in the observation chamber. A two-mode decay is observed with the shorter-lived decay being an unresolved complex possibly having $4p_{1/2}$, Stark-mixed $4p_{3/2}$-$4d_{3/2}$, and Stark-mixed $4f_{5/2}$-$4d_{5/2}$ initial states. (The longest-lived decay of such a complex would be from the fully mixed $4f_{5/2}$-$4d_{5/2}$ initial states having a lifetime of 48 nsec.) Since the $4s$ decay is observed with the proper theoretical lifetime, we assume that the fields existing in the observation chamber are too small to produce appreciable $4s_{1/2}$-$4p_{1/2}$ mixing.

It was necessary to show that the fields existing inside the grounded collision chamber did not appreciably affect the $4s$ data. The collision chamber had been modified to allow a longitudinal electric field to be applied and no measurable change in the $4s$ population could be effected until a field larger than 1 V/cm was applied. However, we would rather base our argument on the fact that the $4s$ atom density followed the expected buildup in the collision chamber for different length chambers, which varied over a factor of 2. The collision chamber was fully grounded for final data.

In principle, a sensitive indicator of mixing is the lifetime of the $4s$ state. The lifetime of the $4p$ state is about 19 times shorter than $4s$, which means that a small amount of mixing can appreciably shorten the "$4s$" lifetime. The effect of Stark mixing has been treated recently (see Wangsness and Series).[3,4] At the risk of being somewhat redundant and since we require slightly different information from that obtained by these authors, we again consider Stark mixing. Using Bethe and Salpeter's notation, we can consider a two-state mixed wave function as

$$U(t)=a_1(t)U_1e^{-i\omega_1t}+a_2(t)U_2e^{-i\omega_2t},$$

where U_2 and U_1 are the field-free unperturbed wave functions. In the atomic system ($e=\hbar=m=1$), we have from time-dependent perturbation theory the following coupled equations:

$$\dot{a}_1=-ifa_2e^{-i\omega t}-2\beta_1a_1,$$
$$\dot{a}_2=-ifa_1e^{i\omega t}-2\beta_2a_2,$$

where f is the electric field perturbation; $\omega=\omega_2-\omega_1$ is the field-free separation of states 1 and 2; and $4\beta_1$ and $4\beta_2$ are the decay rates of states 1 and 2, respectively. The solutions are:

$$e^{-i\omega_1t}a_1=Ae^{\lambda_+t}+Be^{\lambda_-t},$$
$$e^{-i\omega_2t}a_2=Ce^{\lambda_+t}+De^{\lambda_-t},$$

where

$$\lambda_\pm=-\beta_+-\tfrac{1}{2}i(\omega_1+\omega_2)\pm[\beta_-^2-(f^2+\tfrac{1}{4}\omega^2+i\omega\beta_-)]^{1/2}.$$

Here, $\beta_+=\beta_1+\beta_2$, and $\beta_-=\beta_1-\beta_2$. As Bethe and Salpeter do, we define wave functions

$$U_a=(AU_1+CU_2)e^{\lambda_+t},$$
$$U_b=(BU_1+DU_2)e^{\lambda_-t},$$

such that $U(t)$ will be a linear superposition of the U_a and U_b. Letting $\omega\gg f$ and $\omega\gg2\beta_-$, the real part of λ_+ becomes

$$-2\beta_2[1+(\beta_1/\beta_2-1)(f/\omega)^2]$$

which is a measure of the decay rate of state a.

In the limit of $(A/C)^2\approx(f/\omega)^2\ll1$, U_a and U_b are nearly orthogonal. Let state 2 be associated with the $4s_{1/2}$ state, state 1 be associated with the $4p_{1/2}$ state, and state a be associated with the partially mixed $4s_{1/2}$ state. Then

$$\tau_a/\tau_{4s}\approx[1+18(f/\omega)^2]^{-1},$$

where τ_a is the lifetime of state a and τ_{4s} is the lifetime of the field-free $4s$ state.

The excited atom density n^* at the exit aperture of the collision chamber is dependent, in principle, on the lifetime of the state. If cascade is assumed negligible and the gas density is sufficiently low,

$$n^*=Q\rho F\tau(1-e^{-L/v\tau}),$$

where Q is the $4s$ capture cross section, ρ is the gas density in the collision chamber, F is the proton flux, τ is the state lifetime, L is chamber length, and v is the atom velocity. For a uniform field of 1 V/cm which is either parallel or perpendicular to the axis of quantization, $(f/\omega)^2\approx7\times10^{-3}$. Such a field would reduce the $4s_{1/2}$ lifetime by about 13%. The resulting reduction in the $4s$ atom density at the exit aperture would not be detectable in the apparatus since the largest $L/v\tau_{4s}$ value used was about $\frac{1}{3}$. This means that the approximation, $1-e^{-L/v\tau}\approx L/v\tau$, is still fairly good and that the density of the $4s$ atoms at the exit aperture is nearly independent of the lifetime for small fields existing in the chamber. The amount of state mixing depends on $(A/C)^2\approx(f/\omega)^2$ and as long as the capture cross sections into the pure states are comparable, there is little effect on the "cross section" for small fields.

III. APPARATUS

Signal to noise has been increased by cooling the photomultiplier to ice-water temperatures in this experiment. The apparatus is essentially the same as in Ref. 1. The collision chambers were modified to allow a longitudinal electric field to be applied to the collision chamber for other studies. Since data were taken with the chamber grounded, this modification is not important.

[3] R. K. Wangsness, Phys. Rev. **149**, 60 (1966).
[4] G. W. Series, Phys. Rev. **136**, A684 (1964).

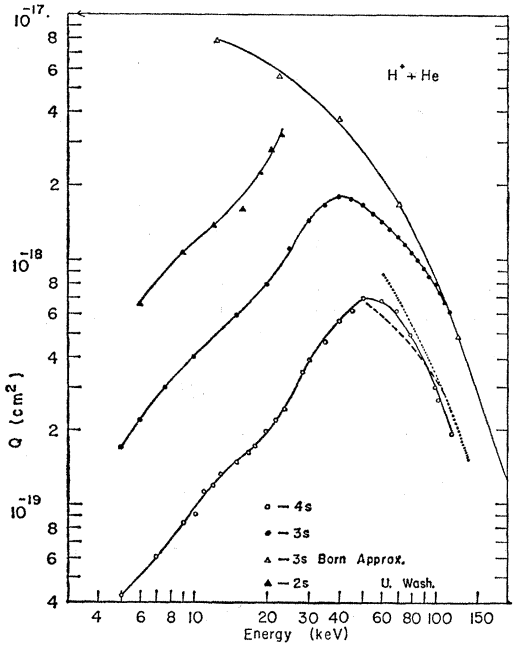

FIG. 2. Plot of $4s$ capture by H^+ on He along with $2s$ (Ref. 8) and $3s$ (Ref. 1) capture. Dotted line is an n^{-3} scaling of the $3s$ Born-approximation curve (Ref. 1) while dashed line is an n^{-3} scaling of the experimental $3s$ curve.

From 5 to 30 keV, data were obtained with the smaller accelerator using an 8-cm-long chamber. A 4-cm chamber was used to verify the proper dependence of the excited atom density on chamber length.

The range 20 to 120 keV was covered with the larger accelerator. Collision chambers of lengths 8 and 18 cm were used to verify the proper buildup with the final data obtained from the 18-cm chamber.

Data on the $4s$ capture were obtained at a distance of $v\tau_{4s}$ from the exit aperture. It was ascertained that this point always fell on an $e^{-x_0/v\tau_{4s}}$ curve, where x_0 is the distance measured from the exit aperture. The $4s$ study required a lengthening of the observation chamber. For example, $v\tau_{4s}$ at 100 keV is 1 m. At such large distances, the spatial beam spread could become a problem but the beam collimation afforded by the longer collision chamber was sufficient to keep all radiating atoms in the field of view.

The H_β filter-lens-photomultiplier system and H_α filter-lens-photomultiplier system were calibrated in the following manner: A hydrogen discharge tube was placed in front of a calibrated spectrometer used in this laboratory.[5] The absolute H_α and H_β emission per steradian from the lamp were recorded. The lamp emissions were scanned around the H_α and H_β wavelengths to determine if there was appreciable molecular background produced by the lamp that might be passed by the Baird-Atomic B1 filters. An appreciable background could not be detected with spectrometer spectral slit widths up to 25 Å. The spectrometer was then removed and a small aperture was placed in the position formerly occupied by the entrance slit of the spectrometer. The filter-lens-photomultiplier system was placed so that a unit-magnified image of the aperture fell on the photo-cathode. (In operation, a unit-magnified image of the beam is projected on the photo-cathode by this optical system.) The H_α and H_β emissions from this aperture were recorded. From the solid angles involved, the sensitivities of the detector systems were determined. The H_α emission from stationary H atoms produced by 100-keV H^+ impact on H_2 was then measured in order to compare with previous measurement.[6] The agreement was within 15%. However, it was decided to normalize to the older measurement so that the most consistent data could be presented from this laboratory. The H_β calibration relative to the normalized H_α calibration was used.

IV. TREATMENT OF DATA

The H_β emissions were measured and the $4s$ cross sections determined by correcting the H_β cross sections according to the proper branching ratio since $4s$ can decay through the $4s \rightarrow 3p$ mode as well as the $4s \rightarrow 2p$ mode.

Since H_α and H_β radiations are produced by reactions with the residual gas in the observation chamber, it was necessary to correct the data by subtracting this background from the total signal. To determine this background the collision chamber was pumped out and gas introduced into the observation chamber until the pressure there was the same as that measured during the actual run. The light signals produced by passing

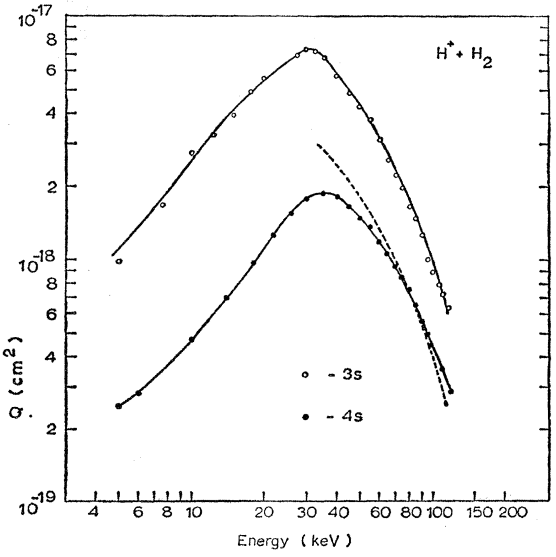

FIG. 3. Plot of $4s$ capture by H^+ on H_2 along with $3s$ capture (Ref. 1). Dashed line represents an n^{-3} scaling of $3s$ capture curve.

[5] R. H. Hughes, R. C. Waring, and C. Y. Fan, Phys. Rev. 122, 525 (1961).

[6] R. H. Hughes, S. Lin, and L. L. Hatfield, Phys. Rev. 130, 2318. (1963)

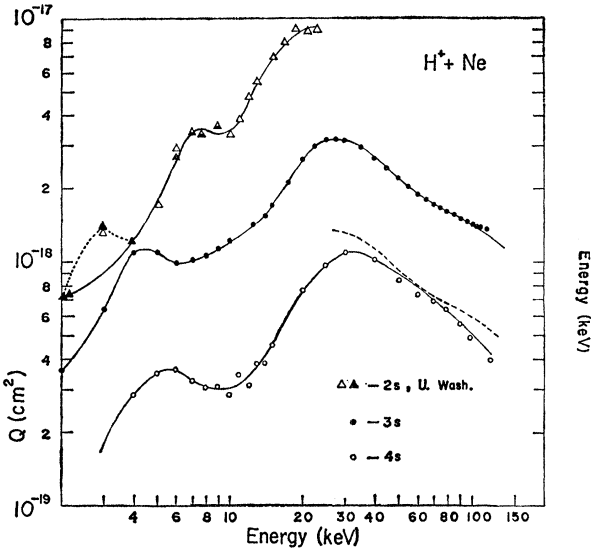

FIG. 4. Plot of 4s capture by H^+ on Ne along with 2s capture (Ref. 8) and 3s capture (Ref. 1). Filled triangles and open triangles represent D^+ and H^+ 2s data, respectively. The dotted 2s curve below 5 keV is our literal interpretation of the 2s data. The dashed line represents an n^{-3} scaling of the 3s curve.

an H^+ beam through the chambers were then measured and taken as background.

The proton flux measured at the Faraday cup was corrected for the beam attenuation due to neutralization in the collision and observation chambers. The beam attenuation was never more than 10%. The mean proton flux in the collision chamber was used in the cross-section determinations.

Reproducibility of data was as follows: 100–120 keV, ±10%; 6–95 keV, ±5%; 5 keV, ±15%.

V. RESULTS AND DISCUSSION

A. Helium

Figure 2 shows a log-log plot of the 4s capture cross section versus proton energy. The 3s capture-cross-section curve also is plotted. This 3s curve is identical with the previously published curve with the exception of adding a point at 120 keV. Also plotted are a 3s curve based on Mapleton's Born-approximation calculations for capture in helium[7] and the 2s capture cross sections measured by Jaecks *et al.*[8]

There is a great similarity among the 2s, 3s, and 4s curve shapes. The maximum in the 4s capture cross section appears to occur nearly 15 keV higher in energy than the 3s maximum. The dashed line in Fig. 2 indicates the 4s cross section calculated by an n^{-3} scaling of the 3s cross section, where n is the principal quantum number. The agreement with the n^{-3} dependence at energies above 80 keV is good where the Born approximation predicts such a dependence.[7,9]

[7] R. A. Mapleton, Phys. Rev. **122**, 528 (1961).
[8] D. Jaecks, B. Van Zyl, and R. Geballe, Phys. Rev. **137**, A340 (1965).
[9] J. D Jackson and H. Schiff, Phys. Rev. **89**, 359 (1953).

B. Hydrogen

Figure 3 is a plot of 4s capture cross section versus proton energy for impact on H_2. The previously published 3s capture-cross-section curve is included. No remeasurements were done on this gas. The curve shapes are similar with a n^{-3} dependence occurring at energies above 60 keV.

Once again the energy at which maximum capture occurs increases with the principal quantum number n. This is a characteristic of all gases studied.

C. Neon

Figure 4 shows the results for Ne. An n^{-3} dependence appears likely to be valid above 50 keV.

Several remeasurements were made on the 3s cross sections with the improved detection systems (cooled photomultiplier). A restudy of the region from 5 to 20 keV resulted in raising the 5-keV point by about 5% and adding a point at 14 keV to the previously published 3s curve. The not-so-evident structure between 6 and 14 keV, which was attributed to possibly the influence of ground-state capture in Ref. 1, was again reproducible. (See Fig. 5, Ref. 1.) Structure between 6 and 14 keV is not evident (or resolved) in the 4s curve. The 3s curve has been extended to 2 keV showing additional structure below 6 keV. A similar structure is indicated in the 4s curve.

It does not seem to us that the influence of ground-state capture is likely to be the entire explanation for the structure below 6 keV in the 3s and 4s curves. Ground-state capture has a reasonable sharp maximum in the vicinity of 10 keV[10] and its influence offers good probable explanation for structure in the range 6–14 keV such as evidenced, in particular, by the 2s curve.

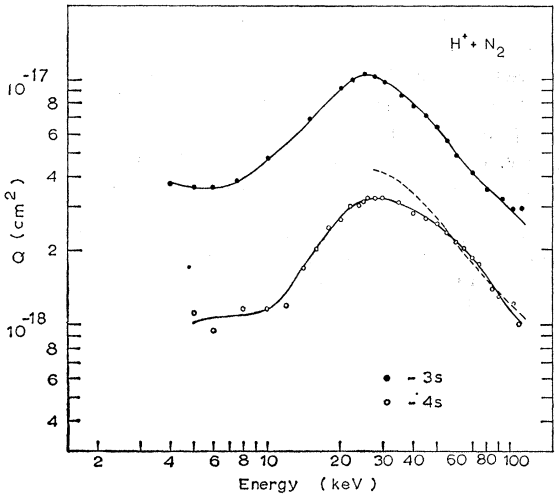

FIG. 5. Plot of 4s capture by H^+ on N_2 along with 3s capture (Ref. 1). Dashed line represents an n^{-3} scaling of 3s curve.

[10] From tabulations of S. K. Allison, Rev. Mod. Phys. **30**, 1137 (1958).

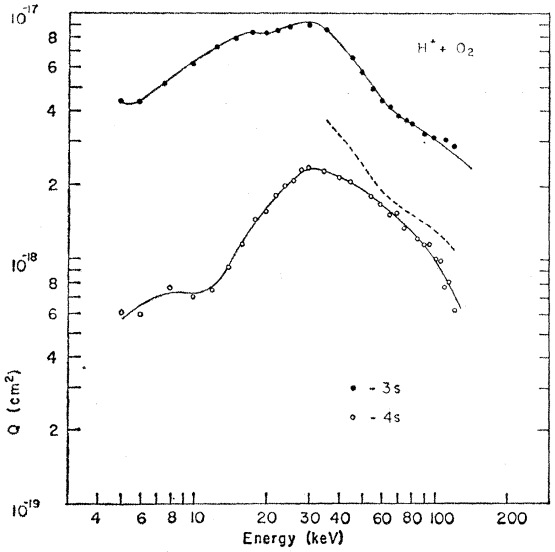

FIG. 6. Plot of 4*s* capture by H^+ on O_2 along with 3*s* capture (Ref. 1). Dashed line represents an n^{-3} scaling of 3*s* curves.

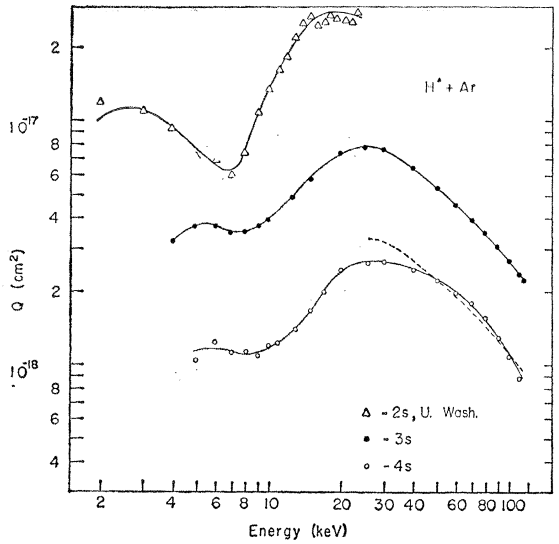

FIG. 7. Plot of 4*s* capture by H^+ on Ar along with 2*s* and 3*s* capture (Refs. 8 and 1, respectively). Dashed line represents an n^{-3} scaling of 3*s* curve.

The secondary maxima in the 3*s* and 4*s* curves occur at energies well below 10 keV and thus the influence of the ground-state capture loses considerable appeal as an explanation. It would seem that University of Washington's 2*s* curve could also be interpreted as having structure below 6 keV. Their published data show points at 3 keV that are definitely above their interpretation of the curve. In Fig. 4 we also dot in a curve which is a literal intepretation of their data.

D. Nitrogen

Figure 5 is a plot of the 3*s* and 4*s* capture cross sections. A 6- and 4-keV point has been added to the previously published 3*s* curve and the 5-keV point has been raised approximately 10%.

The 3*s* and 4*s* curves are similar with the n^{-3} dependence setting in above 50 keV. There is an obvious change in the shape of the curves below 15 keV suggesting additional structure in the curves at lower energies. Unpublished data taken to 2 keV [11] indicate a possible secondary maximum in each curve.

E. Oxygen

Figure 6 is a plot of the 3*s* and 4*s* capture cross section in O_2. A 6-keV point has been added to the previously published 3*s* curve and the 5-keV point has been raised about 5%. Unpublished data to 2 keV [11] indicate a secondary maximum at low energies in each curve.

The agreement with the n^{-3} law at high energies is less striking then in the other gases. This is more likely the result of increased experimental uncertainties brought about by the detrimental effect of this gas on ion gauges, etc. than a failure of the law.

F. Argon

Figure 7 is a plot of the 2*s*, 3*s*, and 4*s* capture cross sections in Ar. The 4-keV point on the 3*s* curve has been raised about 5% relative to the previously published curve while the 2.5- and 3-keV points have been omitted because of the possibility of a systematic error caused by large-angle scattering. Unpublished data to 2 keV [11] indicate a secondary maximum below 8 keV.

[11] Data taken to 2 keV are unpublished because of possible systematic error. For example, the apparent 4*s* cross section for 2-keV impact on N_2 which was obtained from the 8-cm chamber is considerably smaller than from the 4-cm chamber. A possible explanation is that large-angle scattering is occuring and some of the excited atoms are being lost to the inside wall of the chamber. Such measurements cannot be considered absolute and therefore are not included.